

# Charged particle bound orbits around magnetized Schwarzschild black holes: S2 star and hotspot applications

Uktamjon Uktamov<sup>a,b</sup>, Mohsen Fathi<sup>c</sup>, Javlon Rayimbaev<sup>e,d</sup>

<sup>a</sup>*School of Physics, Harbin Institute of Technology, Harbin 150001, People's Republic of China*

<sup>b</sup>*Tashkent University of Applied Sciences, Gavhar Str. 1, Tashkent 100149, Uzbekistan*

<sup>c</sup>*Centro de Investigación en Ciencias del Espacio y Física Teórica, Universidad Central de Chile, La Serena 1710164, Chile*

<sup>d</sup>*Tashkent State Technical University, Tashkent 100095, Uzbekistan*

<sup>e</sup>*National University of Uzbekistan, Tashkent 100174, Uzbekistan*

## Abstract

The dynamics of charged particles around magnetized black holes provide valuable insights into astrophysical processes near compact objects. In this work, we investigate the bound and unbound trajectories of charged particles in the vicinity of a Schwarzschild black hole immersed in an external, uniform magnetic field. By analyzing the effective potential and solving the corresponding equations of motion, we classify the possible orbital configurations and identify the critical parameters governing the transition between stable and escape trajectories. The influence of the magnetic field strength and particle charge on the orbital structure, energy, and angular momentum is systematically explored. Applications of the obtained results are discussed in the context of the S2 star orbiting Sagittarius A\* and the motion of bright hotspots detected near the event horizon, offering a potential interpretation of recent observations in terms of magnetized dynamics. The study contributes to a deeper understanding of charged-particle motion around black holes and its relevance to high-energy astrophysical phenomena in the galactic center.

**Keywords:** Magnetized black holes, charged particle dynamics, bound orbits, S2 star, hotspot motion, galactic center

## 1. Introduction

The motion of charged particles in the vicinity of black holes provides a powerful means of probing the interplay between gravitation, electromagnetism, and relativistic dynamics. The presence of external magnetic fields near compact objects can substantially modify particle trajectories, giving rise to rich orbital structures with direct astrophysical implications [1–9]. Such magnetized environments are expected to occur naturally in accretion flows and jet-launching regions surrounding supermassive black holes, where strong magnetic fields influence both plasma motion and radiation processes [10–16].

Among the simplest yet most instructive models for investigating these effects is the Schwarzschild black hole (SBH) immersed in a uniform magnetic field, often described through Wald's formalism [17–22]. In this configuration, the magnetic field leaves the background geometry unaltered but modifies charged-particle motion via Lorentz interaction. As a result, the corresponding trajectories exhibit intricate dependencies on the particle's charge, energy, angular momentum, and the magnetic field strength. Analyses of such systems not only yield theoretical insights but also offer possible explanations for observed phenomena near black holes, such as quasi-periodic oscillations, flares, and hotspot orbits detected around Sagittarius A\* (Sgr A\*) [23–27].

Recent advances in high-resolution infrared interferometry, particularly through the GRAVITY Collaboration, have enabled precise tracking of the S2 star orbiting Sgr A\* and the detection of compact emission features close to the event horizon [28–33]. These observations open new possibilities for testing relativistic dynamics in strong-gravity regimes. The study of charged-particle motion in magnetized black-hole spacetimes provides a useful theoretical framework for interpreting such data, offering constraints on the local magnetic-field distribution, plasma properties, and the possible charge-to-mass ratios of radiating particles.

In this work, we analyze the bound and unbound trajectories of charged particles in a Schwarzschild spacetime embedded in an external, asymptotically uniform magnetic field. Using the Hamilton–Jacobi formalism, we derive the equations of motion and examine the structure of the corresponding effective potential, identifying the regions of stable, unstable, and escape orbits. The influence of the magnetic-field parameter and the particle's charge on the critical radii of circular motion, including the innermost stable circular orbit (ISCO), is explored in detail.

Furthermore, we apply the obtained results to two astrophysical contexts: (i) the orbital dynamics of the S2 star in the galactic center, and (ii) the motion of bright hotspots observed near Sgr A\*, whose periodic variability may reflect the effects of magnetized dynamics. We also employ the Levin–Perez–Giz (LP) taxonomy of relativistic orbits [34–40] to classify bound trajectories in the magnetized Schwarzschild background.

*Email addresses:* uktam.uktamov11@gmail.com (Uktamjon Uktamov), mohsen.fathi@central.cl (Mohsen Fathi), javlon@astrin.uz (Javlon Rayimbaev)

The remainder of this paper is organized as follows. In Sect. 2, we present the SBH spacetime immersed in a magnetic field and derive the equations of motion using the standard Lagrangian formalism, which are then analyzed for orbital stability. We subsequently constrain the magnetic parameter of the model in accordance with the observed orbital characteristics of the S2 star around Sgr A\*. In Sect. 3, we explore the influence of different magnetic-field strengths on the bound motion of charged particles and provide numerical simulations of the corresponding trajectories. Finally, our conclusions are summarized in Sect. 4.

In this work, we employ natural units ( $G = c = 1$ ), adopt the metric signature  $(-, +, +, +)$ , and use primes to indicate derivatives with respect to the radial coordinate.

## 2. Charged Particle Dynamics around SBHs in a Magnetic Field

We consider a SBH described by the line element

$$ds^2 = -f(r)dt^2 + f(r)^{-1}dr^2 + r^2d\Omega^2, \quad (1)$$

in the standard Schwarzschild coordinates  $x^\alpha = (t, r, \theta, \phi)$ , where  $d\Omega^2 = d\theta^2 + \sin^2\theta d\phi^2$ . The lapse function is given by

$$f(r) = 1 - \frac{2M}{r}. \quad (2)$$

The black hole is immersed in an external, asymptotically uniform magnetic field of strength  $B$ . Following Wald's prescription [17], the electromagnetic four-potential is expressed as  $A^\mu = \frac{B}{2}\xi_\phi^\mu$ , with  $\xi_\phi^\mu = (0, 0, 0, 1)$  representing the azimuthal Killing vector. Consequently, the only non-zero covariant component of the potential is

$$A_\phi = \frac{1}{2}Br^2 \sin^2\theta. \quad (3)$$

### 2.1. Equations of motion

The motion of a charged particle with mass  $m$  and electric charge  $q$  is derived from the Lagrangian

$$\mathcal{L} = \frac{1}{2}mg_{\mu\nu}u^\mu u^\nu + qA_\mu u^\mu, \quad (4)$$

and equivalently from the Hamilton-Jacobi equation [7]:

$$g^{\mu\nu} \left( \frac{\partial S}{\partial x^\mu} - qA_\mu \right) \left( \frac{\partial S}{\partial x^\nu} - qA_\nu \right) = -m^2, \quad (5)$$

where the action is  $S = -Et + L\phi + S_\theta(\theta) + S_r(r)$ . Confining motion to the equatorial plane ( $\theta = \pi/2$ ), the equations of motion reduce to

$$\dot{t} = \frac{\mathcal{E}}{f(r)}, \quad (6a)$$

$$\dot{\phi} = \frac{l}{r^2} - \beta, \quad (6b)$$

$$\dot{r}^2 = \mathcal{E}^2 - V_{\text{eff}}(r), \quad (6c)$$

where  $\mathcal{E} = E/m$  is the specific energy,  $l = L/m$  is the specific angular momentum, and  $\beta = qB/(2m)$  is the magnetic parameter. Hence, the radial motion as a function of  $\phi$  is governed by

$$\left( \frac{dr}{d\phi} \right)^2 = \left( \frac{r^2}{l - \beta r^2} \right)^2 [\mathcal{E}^2 - V_{\text{eff}}(r)] := P(r), \quad (7)$$

in which, the effective potential is

$$V_{\text{eff}}(r) = f(r) \left[ 1 + \left( \frac{l}{r} - \beta r \right)^2 \right]. \quad (8)$$

### 2.2. Circular orbits and stability

Figure 1 shows the effective potential  $V_{\text{eff}}(r)$  as a function of  $r$ . Minima correspond to stable circular orbits (red points), and maxima correspond to unstable orbits (gray points). For  $\beta > 0$ , the Lorentz force is repulsive, reducing the radius of unstable orbits, while  $\beta < 0$  increases it due to attraction.

In general, the specific angular momentum  $l$  and specific energy  $\mathcal{E}$  for circular orbits of radius  $r_c$  are obtained from  $\mathcal{E}_c^2 = V_{\text{eff}}(r_c)$  and  $V'_{\text{eff}}(r_c) = 0$ :

$$l_c = \frac{r_c \left[ \sqrt{\beta^2 r_c^4 f(r_c)^2 + M(r_c - 3M)} - \beta M r_c \right]}{r_c - 3M}, \quad (9)$$

$$\mathcal{E}_c^2 = f(r_c) \left[ 1 + \frac{\left( \sqrt{\beta^2 r_c^4 f(r_c)^2 + M(r_c - 3M)} - \beta r_c^2 f(r_c) \right)^2}{(r_c - 3M)^2} \right]. \quad (10)$$

In Fig. 2, we show the relationship between  $\mathcal{E}_c$  and  $l_c$  for different values of the magnetic parameter  $\beta$ .

Moreover, the innermost stable circular orbit (ISCO) is defined by  $V''_{\text{eff}} = 0$ , with stable orbits satisfying  $V''_{\text{eff}} > 0$  and unstable ones satisfying  $V''_{\text{eff}} < 0$ . Table 1 lists the critical radii for three values for  $\beta$ , showing the impact of this parameter on the critical radius. Figure 3 illustrates the dependence of the

$\beta$	$r_{\text{ISCO}}$
-0.01	5.85955M
0.0	6M
0.01	5.8414M

Table 1: Critical radii of circular orbits for different values of the magnetic parameter  $\beta$ .

critical radius on  $\beta$ , along with the corresponding constants of motion at the ISCO.

### 2.3. Applications to hotspot orbits around Sgr A\*

Using GRAVITY data [29], the orbital period  $T$  of a charged particle on a circular orbit is

$$T = \frac{2\pi}{\Omega_K}, \quad (11)$$

where

$$\Omega_K = \frac{\dot{\phi}}{\dot{t}} = \frac{f(r)(l - \beta r^2)}{r^2 \mathcal{E}_c}, \quad (12)$$

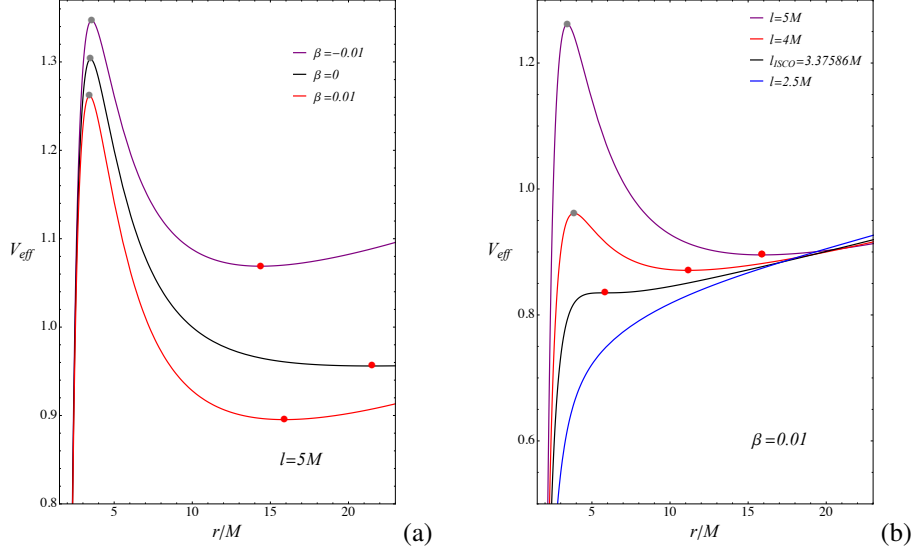


Figure 1: Effective potential  $V_{\text{eff}}(r)$  for charged particles near a SBH: (a) varying  $\beta$  with fixed  $l$ , and (b) varying  $l$  with fixed  $\beta$ . Red points correspond to stable circular orbits, gray points to unstable orbits.

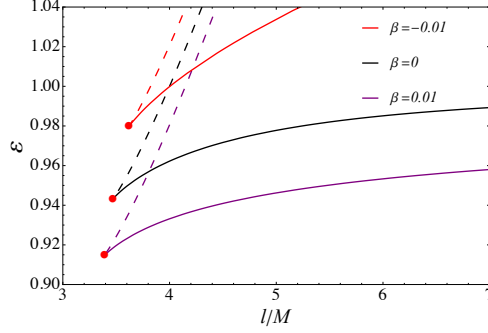


Figure 2: Specific energy  $\mathcal{E}_c$  versus angular momentum  $l_c$  for circular orbits. Solid lines indicate stable orbits, dashed lines indicate unstable orbits. Red points mark the ISCO (see also Table 1).

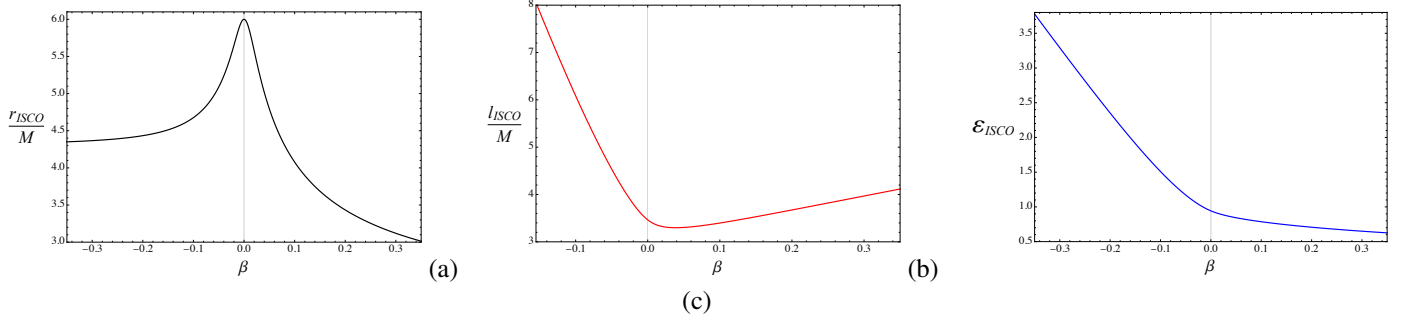


Figure 3: Dependence of ISCO parameters on  $\beta$ : (a) radius  $r_{\text{ISCO}}$ , (b) angular momentum  $l_{\text{ISCO}}$ , and (c) energy  $\mathcal{E}_{\text{ISCO}}$ .

with  $l_c$  and  $\mathcal{E}_c$  given by Eqs. (9) and (10). Figure 4 shows the period as a function of orbital radius for different  $\beta$ , constraining  $-0.0011 < \beta < -0.00065$  for Sgr A\* with  $M = 4.14 \times 10^6 M_\odot$ .

### 3. Relativistic bound orbits and LP taxonomy

To analyze the bound motion of charged particles, we employ the LP taxonomy [34], which allows us to determine the specific

energy  $\mathcal{E}$  and specific angular momentum  $l$  for a given orbit. From Eq. (7), bound orbits satisfy  $P(r) = 0$ , whose two roots can be expressed as

$$r_1 = \frac{\lambda}{1-e}, \quad r_2 = \frac{\lambda}{1+e}, \quad (13)$$

where  $\lambda$  and  $e$  are the latus rectum and eccentricity of the orbit, respectively [41].

Using Eq. (7), the specific angular momentum and energy of a charged particle corresponding to a given  $(\lambda, e)$  are obtained

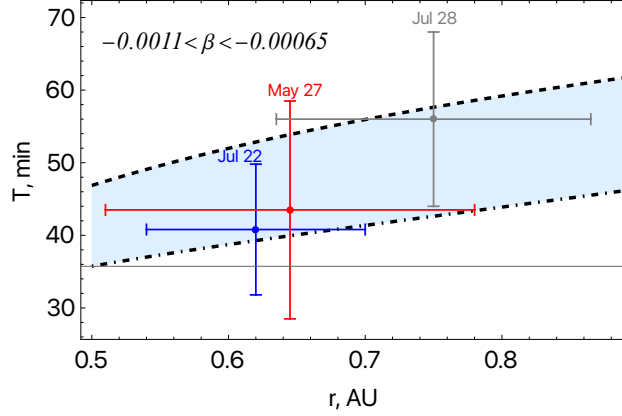


Figure 4: Orbital period  $T$  versus radius for various magnetic parameters  $\beta$ .

as

$$l = \frac{\mathcal{A} - \mathcal{B}}{\Psi}, \quad (14)$$

$$\mathcal{E} = \frac{1}{\Psi} \sqrt{\frac{\mathcal{C}(\mathcal{D} + \mathcal{E} + \mathcal{H} - \lambda)}{\Xi}}, \quad (15)$$

where the definitions of  $\mathcal{A}$ ,  $\mathcal{B}$ ,  $\mathcal{C}$ ,  $\mathcal{D}$ ,  $\mathcal{E}$ ,  $\mathcal{H}$ ,  $\Psi$ , and  $\Xi$  are provided in [Appendix A](#).

Assuming that the particle begins at  $r = r_1$  and  $\phi = 0$ , the evolution of the azimuthal angle over one period is

$$q + 1 = \frac{\Delta\phi}{2\pi} = \frac{1}{\pi} \int_{r_1}^{r_2} \frac{dr}{\sqrt{P(r)}}, \quad (16)$$

where  $q = \omega + v/z$  characterizes the orbit shape, with  $\omega$ ,  $v$ , and  $z$  representing the whirl, vertex, and zoom numbers. The latus rectum  $\lambda$  for a chosen trajectory is obtained by numerically integrating Eq. (16) and applying the bisection method to determine its precise value.

Table 2 provides representative numerical values of the latus rectum  $\lambda$ , specific angular momentum  $l$ , and specific energy  $\mathcal{E}$  for selected eccentricity  $e$  and magnetic parameter  $\beta$ . These parameters correspond to the periodic orbits chosen according to the LP classification.

$(z, \omega, v)$	$\beta$	$e$	$\lambda$	$l$	$\mathcal{E}$
(1,0,1)	-0.01	0.8	7.57692M	4.53508M	1.08749
(1,0,1)	0.0	0.8	8.56483M	3.85943M	0.98033
(1,0,1)	0.001	0.8	8.27243M	3.83679M	0.97681
(2,0,1)	-0.01	0.8	9.43026M	5.14769M	1.13158
(2,0,1)	0.0	0.8	11.145M	4.06822M	0.98450
(2,0,1)	0.001	0.8	9.69877M	3.93809M	0.97969
(3,0,1)	-0.01	0.8	11.2205M	6.01062M	1.18105
(3,0,1)	0.0	0.8	13.9918M	4.34877M	0.98751
(3,0,1)	0.001	0.8	10.7349M	4.03252M	0.98142
(4,0,1)	-0.01	0.8	12.8577M	7.00283M	1.23147
(4,0,1)	0.0	0.8	16.9124M	4.64228M	0.98959
(4,0,1)	0.001	0.8	11.4448M	4.10277M	0.98247

Table 2: Specific energy  $\mathcal{E}$  and specific angular momentum  $l$  for selected eccentricity  $e$  and periodic orbits, with fixed values of the magnetic parameter  $\beta$ .

### 3.1. Representative orbits

Figure 5 shows the selected bound orbits for various  $(z, \omega, v)$  and magnetic parameters  $\beta$ . The black hole is located at the origin, and the effect of the magnetic field on the shape and extent of the orbits is evident.

## 4. Conclusions

In this work, we have investigated the motion of charged particles in the Schwarzschild spacetime embedded in a uniform external magnetic field, following Wald's prescription. By deriving and analyzing the effective potential and the corresponding equations of motion, we identified the key dynamical features governing both circular and noncircular trajectories. The stability analysis of circular motion revealed that the magnetic coupling parameter  $\beta$  plays a decisive role in modifying the location of the ISCO, as well as the associated constants of motion.

The study further explored the astrophysical implications of these results in two important observational contexts: the orbital motion of the S2 star and the near-horizon dynamics of bright hotspots detected around Sgr A\*. By constraining the allowed values of  $\beta$  through GRAVITY observational data, we demonstrated that small magnetic couplings can produce measurable deviations in the orbital period, offering a potential explanation for magnetically induced perturbations in stellar and plasma trajectories near the galactic center.

Using the LP taxonomy, we classified relativistic bound trajectories and provided numerical examples illustrating the influence of  $\beta$  and eccentricity  $e$  on orbital morphology. The obtained family of periodic and quasiperiodic solutions highlights how weak magnetization can lead to distinctive zoom-whirl structures and nontrivial precession patterns, potentially observable through high-precision astrometric monitoring.

To summarize, our results underline the importance of magnetic effects in shaping the relativistic dynamics of charged particles near black holes. Future extensions of this work may include the consideration of rotating (Kerr) geometries, plasma backreaction, and radiative energy losses, thereby offering a

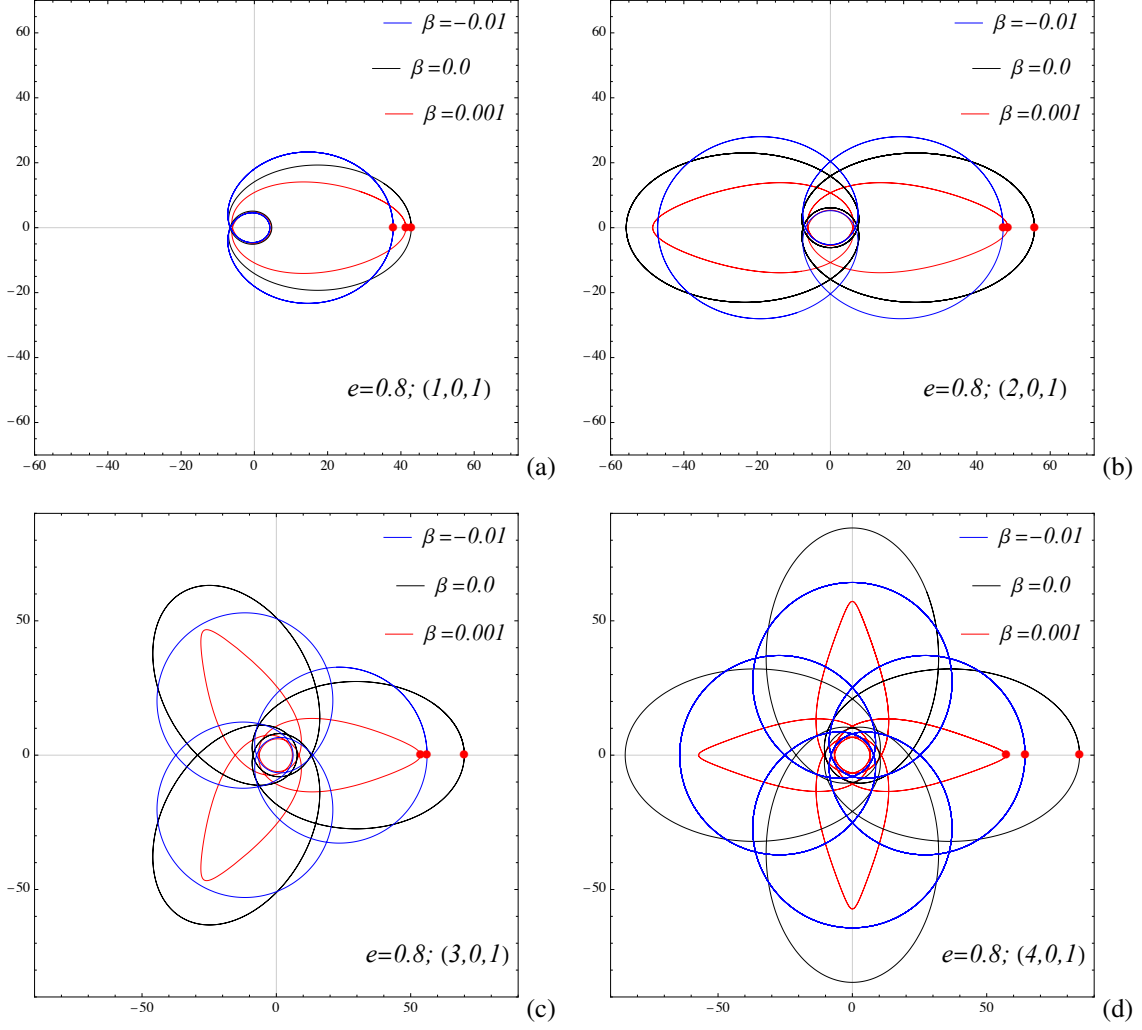


Figure 5: Bound orbits of charged particles for selected  $(z, \omega, \nu)$  and fixed magnetic parameter  $\beta$ . The black hole is at the origin.

more complete description of magnetized accretion and emission phenomena in strong-gravity environments.

### Acknowledgements

The work of M.F. has been supported by Universidad Central de Chile through the project No. P Ducen20240008.

### Appendix A. The coefficients in Eqs. (14) and (15)

These coefficient are as follows:

$$\mathcal{A} = \lambda^2 M \beta (1 - e^2)^2, \quad (\text{A.1})$$

$$\mathcal{B} = \left\{ (1 - e^2)^2 \lambda^2 \left[ \beta^2 \lambda^4 - (1 - e^2) M^2 (4\beta^2 \lambda^2 + e^4 + 2e^2 - 3) + \lambda M (-4\beta^2 \lambda^2 + e^4 - 2e^2 + 1) \right] \right\}^{1/2}, \quad (\text{A.2})$$

$$\Psi = (1 - e^2)^2 [(e^2 + 3)M - \lambda], \quad (\text{A.3})$$

$$\mathcal{E} = 4(1 - e^2)M^2 - \lambda^2 + 4\lambda M, \quad (\text{A.4})$$

$$\mathcal{D} = \lambda (-2\beta^2 \lambda^2 - e^4 - 2\beta^2 e^2 \lambda^2 + 2e^2), \quad (\text{A.5})$$

$$\mathcal{E} = 2\beta \left\{ (1 - e^2)^2 \lambda^2 \left[ \beta^2 \lambda^4 - (1 - e^2) M^2 (4\beta^2 \lambda^2 + e^4 + 2e^2 - 3) + \lambda M (-4\beta^2 \lambda^2 + e^4 - 2e^2 + 1) \right] \right\}^{1/2}, \quad (\text{A.6})$$

$$\mathcal{H} = M \left[ 4\beta^2 \lambda^2 + e^6 + e^4 + e^2 (12\beta^2 \lambda^2 - 5) + 3 \right], \quad (\text{A.7})$$

$$\Xi = (e^2 + 3)M - \lambda. \quad (\text{A.8})$$

## References

- [1] V. P. Frolov and A. A. Shoom, *Phys. Rev. D* **82**, 084034 (2010).
- [2] Y.-K. Lim, *Phys. Rev. D* **91**, 024048 (2015).
- [3] A. Tursunov, Z. Stuchlík, and M. Kološ, *Phys. Rev. D* **93**, 084012 (2016).
- [4] B. Narzilloev, A. Abdujabbarov, C. Bambi, and B. Ahmedov, *Phys. Rev. D* **99**, 104009 (2019).
- [5] F. Abdulxamidov *et al.*, *Phys. Rev. D* **108**, 044030 (2023).
- [6] J. M. Ladino, C. A. Benavides-Gallego, *et al.*, *Eur. Phys. J. C* **83**, 989 (2023).
- [7] U. Uktamov, M. Alloqulov, S. Shaymatov, T. Zhu, and B. Ahmedov, *Phys. Dark Univ.* **47**, 101743 (2025), [arXiv:2412.01809 \[gr-qc\]](#).
- [8] U. Uktamov, M. Fathi, J. Rayimbaev, and A. Abdujabbarov, *Phys. Rev. D* **110**, 084084 (2024), [arXiv:2406.03371 \[gr-qc\]](#).
- [9] T. Oteev *et al.*, *Eur. Phys. J. C* **85**, 953 (2025).
- [10] J. C. McKinney *et al.*, *Monthly Notices of the Royal Astronomical Society: Letters* **454**, L6 (2015).
- [11] B. Sarkar and S. Das, *Monthly Notices of the Royal Astronomical Society* **461**, 190 (2016).
- [12] B. Ripperda *et al.*, *The Astrophysical Journal Letters* **914**, L1 (2022).
- [13] A. Janiuk *et al.*, *Astronomy & Astrophysics* **668**, A66 (2022).
- [14] B. Crinquand *et al.*, *Physical Review Letters* **129**, 205101 (2022).
- [15] A. Nathanail *et al.*, *Astronomy & Astrophysics* **518**, A36 (2025).
- [16] K. Chatterjee *et al.*, *Physical Review D* **112**, 063013 (2025).
- [17] R. M. Wald, *Phys. Rev. D* **10**, 1680 (1974).
- [18] D. V. Gal'tsov, *Soviet Physics JETP* **47**, 419 (1978).
- [19] A. Tursunov *et al.*, *Physical Review D* **87**, 125003 (2013).
- [20] M. Kološ *et al.*, *Classical and Quantum Gravity* **32**, 165009 (2015).
- [21] J. Rayimbaev *et al.*, *Physics of the Dark Universe* **45**, 101516 (2024).
- [22] J. Rayimbaev *et al.*, *Universe* **9**, 135 (2023).
- [23] Z. Stuchlík *et al.*, *Astronomy & Astrophysics* **551**, A24 (2013).
- [24] X. Lin *et al.*, *Monthly Notices of the Royal Astronomical Society* **520**, 1271 (2023).
- [25] N. Aimar *et al.*, *Astronomy & Astrophysics* **670**, A30 (2023).
- [26] B. Rahmatov *et al.*, *Chinese Journal of Physics* **92**, 143 (2024).
- [27] A. Levis *et al.*, *Nature Astronomy* **8**, 123 (2024).
- [28] R. Abuter *et al.*, *Astronomy & Astrophysics* **615**, L15 (2018).
- [29] R. Abuter *et al.*, *Astronomy & Astrophysics* **618**, L10 (2018).
- [30] R. Abuter *et al.*, *Astronomy & Astrophysics* **636**, L5 (2020).
- [31] R. Abuter *et al.*, *Astronomy & Astrophysics* **647**, A59 (2021).
- [32] I. D. Martino *et al.*, *Physical Review D* **104**, L101502 (2021).
- [33] GRAVITY Collaboration, O. Straub, *et al.*, *A&A* **672**, A63 (2023).
- [34] J. Levin and G. Perez-Giz, *Physical Review D* **77**, 103005 (2008).
- [35] G. Perez-Giz and J. Levin, *Physical Review D* **79**, 124013 (2009).
- [36] G. Perez-Giz and J. Levin, *Physical Review D* **79**, 124014 (2009).
- [37] V. Misra and G. Perez-Giz, *Physical Review D* **82**, 083001 (2010).
- [38] R. Grossman *et al.*, *Phys. Rev. D* **85**, 023012 (2012).
- [39] B. Gao and X.-M. Deng, *Annals of Physics* **418**, 68194 (2020).
- [40] Y.-K. Lim and Z. C. Yeo, *Phys. Rev. D* **109**, 024037 (2024).
- [41] S. Chandrasekhar, *The mathematical theory of black holes*, Vol. 69 (Oxford university press, 1998).